



## Synthesis and Characterization of Quaternary Chalcogenide Nanomaterials: A Review Study

Huda Talib<sup>1\*</sup>, Nabeel A. Bakr<sup>1</sup>, Mohammed A. Abed<sup>2</sup>

<sup>1</sup>Department of physics, College of Science, University of Diyala, Diyala, Iraq

<sup>2</sup>Diyala Directorate General of Education, Diyala, Iraq

[sciphys2125@uodiyala.edu.iq](mailto:sciphys2125@uodiyala.edu.iq)

Received: 28 August 2022

Accepted: 27 December 2022

DOI: <https://doi.org/10.24237/ASJ.02.01.676C>

### Abstract

For the past ten years, copper-based quaternary chalcogenide semiconductor materials have also been studied and classified in a variety of ways. The majority of research and academic works on quaternary chalcogenides are devoted to solar cell PV studies, where, as the material first gained popularity as a less expensive option in contrast to Si for Solar PV systems. . Such components have all of the desirable characteristics for becoming an effective PV material in the thin films or nanomaterials configuration, like effective and non-toxic unique materials, effective charge carrier, best possible energy band, as well as higher adsorption co-effectiveness.  $Cu_2MIMIIIX_4$  (where X = S or/and Se; MII = Si, Sn, and Ge; MI = Zn, Mn, Fe, Co, Ni, Cd, and Hg) is a new class of quaternary materials that has just emerged and found use in electrochemistry, thermal, sensor systems, power banks, and some other technologies. The unique combination characteristics of this class of chalcogenides, like optoelectronic and electrical; magnetic and optoelectronic; as well as thermo-electric, make their potentially useful importance for a variety of usages. Even though many of the papers have already covered the PV characteristics of such quaternary chalcogenides, this material has many various uses that remain investigated. This article touches on the multi-functional systems of novel dissimilar quaternary copper-based chalcogens, including the fabrication, the doping impact on their physical and chemical characteristic, and their use in many applications, including solar cells.



**Keywords:** Quaternary chalcogenide, Quaternary semiconductor, Stannite structure, Kesterite structure.

## تركيب وخصائص المواد النانوية الكلوكونينية الرباعية: دراسة مرجعية

هدى طالب جليل<sup>1</sup>، نبيل علي بكر<sup>1</sup>، محمد علي عبد<sup>2</sup>

<sup>1</sup> قسم الفيزياء - كلية العلوم - جامعة ديالى

<sup>2</sup> المديرية العامة للتربية في ديالى

### الخلاصة

على مدار السنوات العشر الماضية، تمت دراسة وتصنيف مواد أشباه الموصلات الرباعية المعتمدة على الكالكونينيدات النحاسية بطرائق عدة. ان غالبية الاعمال الاكاديمية البحثية حول الكالكونينيدات الرباعية مكرسة لدراسة الخلايا الشمسية الكهروضوئية، اذ اكتسبت المادة شعبية لاول مرة كخيار اقل تكلفة على عكس انظمة الخلايا الشمسية الكهروضوئية المعتمدة على السليكون. تتمتع هذه المكونات بجميع الخصائص المرغوبة لتصبح مادة كهروضوئية فعالة في تكوين تركيب الاغشية الرقيقة او المواد النانوية، مثل المواد الفريدة غير السامة، وحامل الشحنة الفعالة، وافضل حزمة طاقة ممكنة، فضلا عن الكفاءة المشتركة للامتصاص.  $Cu_2MIMIX_4$  (حيث  $X = S$  أو  $Se$ ؛  $MII = Si$  و  $Sn$  و  $Ge$  و  $MI = Zn$  و  $Mn$  و  $Fe$  و  $Co$  و  $Ni$  و  $Cd$  و  $Hg$ ) هي فئة جديدة من المواد الرباعية التي ظهرت للتو وطبقت في تطبيقات التحفيز الحراري الكهربائي، وانظمة الاستشعار وبنوك الطاقة وبعض التقنيات الاخرى. الخصائص المركبة الفريدة لهذه الفئة من الكالكونينيدات، كخصائصها الالكترونية البصرية والكهربائية؛ المغناطيسية الالكترونية والبصرية؛ فضلا عن الكهروحرارية والكهربائية، تجعل اهميتها مفيدة لمجموعة متنوعة من الاستعمالات. على الرغم من ان العديد من البحوث قد غطت بالفعل الخصائص الكهروضوئية لمثل هذه الكالكونينات الرباعية، الا انه لم يتم دراسة العديد من الاستعمالات المختلفة لهذه المواد. يتطرق البحث الحالي الى الانظمة متعددة الوظائف للكالكونينات النحاسية غير المتشابهة الجديدة القائمة على النحاس، بما في ذلك التصنيع، وتأثير التشويب على خصائصها الفيزيائية والكيميائية ومجالات استعمالها مع مجموعة متنوعة من لتطبيقات، بما في ذلك الخلايا الكهروضوئية.

**كلمات مفتاحية:** كالكونينيد الرباعي، أشباه الموصلات الرباعية، هيكل ستانيت، هيكل كيستريت.

### Introduction

Photovoltaics with a low cost are necessary to improve the efficiency of today's thin-film solar power cells. As a result, most solar cells made of chalcopyrite thin film ( $CuIn_xGa_{1-x}S$ ) ( $Se$ )<sub>2</sub> (CIGS) are theoretically compared to conventional silicon PV cells. [1–3]. It is important to

remember that these materials are only effective at 23.35% [4]. Furthermore, these materials have grown prohibitively expensive, causing scarcity and significant environmental impact.. Quaternary chalcogenide semiconductors are an uncommon and potentially useful replacement for the absorbent layers found in traditional unsafe solar cells (I2-II-IV-VI4). I: copper and silver; II: zinc, cadmium, iron, and manganese; IV: silicon, germanium, and tin; VI: sulfur and selenium. Their greatest attribute is their non-toxicity and ease of accessibility on Earth. These semiconductors, which have already shown an astounding 10% efficiency in solar cells, have many more applications and other uses [5–13]. In-depth research has been conducted on the classification of the constituents, kesterites such as  $\text{Cu}_2\text{ZnSnS}_4$  (CZTS); as well as stannites such as  $\text{Cu}_2\text{FeSnS}_4$  (CFTS) [14, 15].  $\text{Cu}_2\text{MnSnS}_4$  (CMTS), a fabricated stannite-type material, has also experienced wide characterization. As feasible photovoltaic systems, CMTS and CFTS are recommended due to their more suitable energy band gap and optical characteristics [16]. To produce these materials, many methods were developed [17–28]. An earlier review study discussed many methods for doing this [29], may require various lengths of time for synthesis (the liquid reflux process, for instance, needs 6–12 hours) [21], Microwave-based synthesis requires five minutes of irradiation [18], while Sonochemical synthesis requires three hours[30]. Several of these methods necessitate further thermal treatment [30]. Fig. 1 depicts the formation of tertiary and quaternary chemicals by a zinc buckle [31].

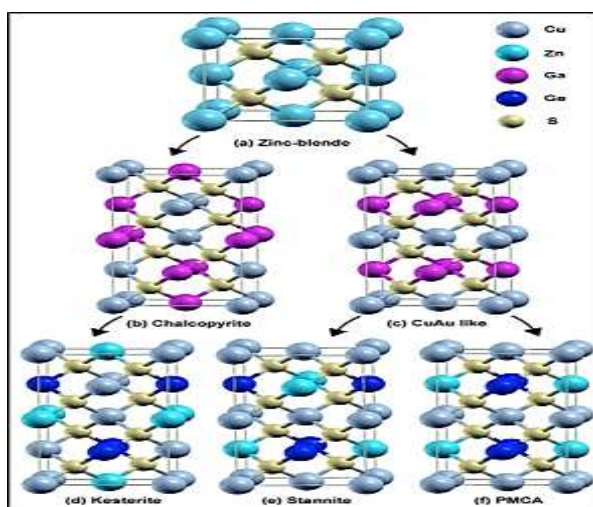


**Figure 1:** Formation of quaternary and tertiary compounds from zinc buckle.

Considering the discovery of numerous chemical and physical formulation technologies for fabrication of the mass bulk, powder, layers of thin film, as well as nanostructures, the preparation of these complex quaternary chalcogenides has developed. Simplified methods concerning film development like as a successive ionic layer, vapor deposition, and nanostructured ink deposition; have similarly developed alongside more complicated physical techniques [32–35]. Fig. 2. illustrates several of these methods to manufacture a quaternary crystalline chalcogenide nanomaterial on the substrates. These techniques can use to create a wide range of photovoltaic and sensor devices, as well as photocatalyst electrodes. Over time, several methods of chemistry fabrication, including Microwave-reactions produce, sol-gel, high-pressure homogenization, hydrothermal processes, and sophisticated thermally resistant colloid formation technologies have constituted.

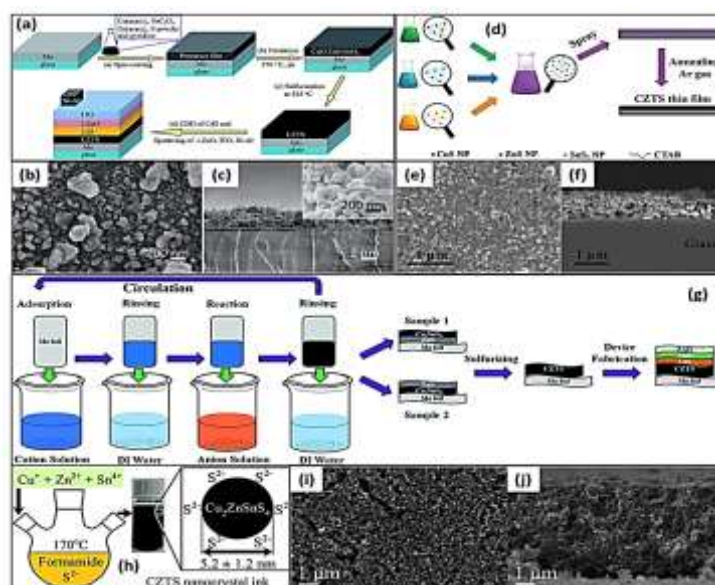


**Figure 2:** Shows how to deposit quaternary chalcogenides in thin films. (a) a diagram for a solar cell with CZTS, ITO, i-ZnO, CdS, NiAl, and Mo-coated glass substrate, using an air-stable molecule preparatory ink. (b and c) CZTS film analyzed via surfaces and cross-section morphologies; insets show proportionally enlarged SEM images. (d) CZTS thin films are synthesized utilizing SnS<sub>2</sub>, CuS, and ZnS nanopowders and imaged with a scanning electron microscope after annealing at 400°C. (e) The level surface view displays the CZTS thin film



that has been prepared. (f) Cross-sectional image presentation view. (g) A diagram depicting the flexible photovoltaic modules made of CZTS material mounted on a sheet of Mo foil. (h) An example ink made using CZTS nanocrystals production with a suggestion for stabilizing the nanocrystals' dispersion in formamide. (i- j) A film of CZTS FA nanocrystals is shown in SEM images from both the top and cross-section. [32–35].

Currently, chemical synthesis techniques are preferred method for manufacture the nanocrystalline structures of such materials particularly quaternary chalcogenides.. The high-temperature colloidal production method and its hydro/solvothermal technologies are generally used for the production of morphologically and chemically diverse nanostructured quaternary chalcogenides. Fig. 3 illustrates various chemical production techniques used to manufacture quaternary chalcogenides. Naturally, Nanoparticles can be synthesized using a high-thermal colloidal method, (Figure 4 illustrates the process of creating thermal-resistant colloids schematically). The process involves heating different material components such as acetates, nitrates, acetylacetonates, or chlorides to a high reflux temperature (usually 200-300 °C). Organic ligands or capping agents such as oleylamine, octadecene, or oleic acid are used to increase the melting and boiling points of the solutes. Long-chain thiols, amines, and phosphonic acids with comparable structures, such as trioctylphosphine (TOP), trioctylphosphine oxide (TOPO), and others are also used. The size and shape of the nanoparticles can be controlled using a capping agent. The quantum captivity system of nanoparticles exhibits substantial optical tuning on size change [36, 37]. To achieve high purity levels of nanomaterials, it is customary to use inert conditions. The Quaternary CZTX (where X can be Se or S) nanoparticles were initially produced through a colloidal synthesis method. Shannon et al., Riha et al., Steinhagen et al., and Ibaez et al. were among the researchers who employed this technique [9, 38-39]. First, using a colloidal synthesis technique, Shavel et al. produced  $Cu_2Zn_xSnySe_{1+x+2y}$  formatting non-asymmetrical [10]. Fig. 5. shows some of the intriguing nanoscale materials produced for different uses using the colloidal synthesis technique.

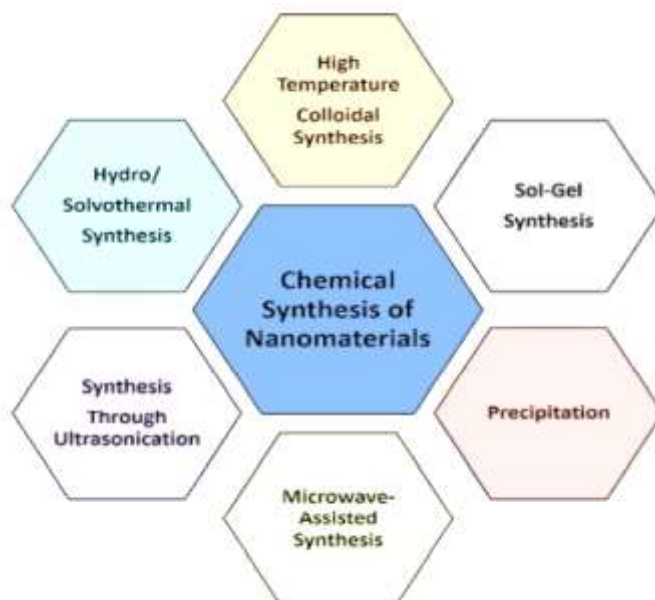


**Figure 3:** Various techniques used to produce quaternary chalcogenides chemically.

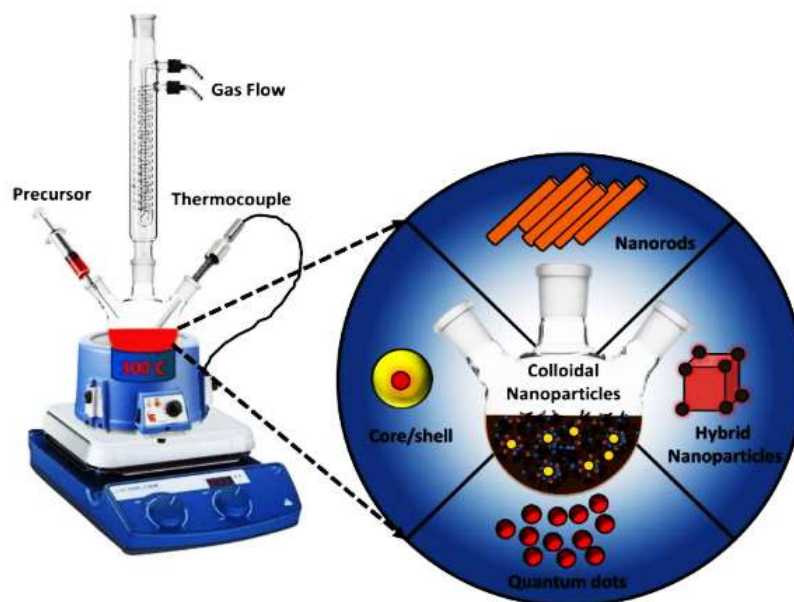


**Figure 4:** The fabrication of thermal-resistant colloids procedure schematically.

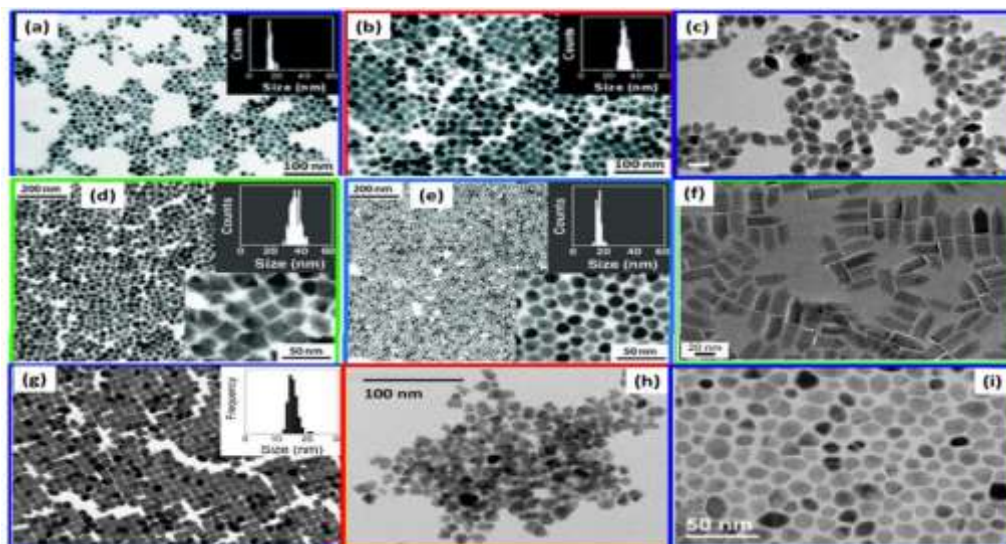


**Figure 5:** Characteristic TEM images of Cu-based quaternary chalcogenide nanostructures as they were discovered (a)  $\text{Cu}_2\text{HgSnSe}_4$ , (b)  $\text{Cu}_{2.3}\text{Hg}_{0.7}\text{SnSe}_{3.8}$ , (c) non-stoichiometric polytypic  $\text{Cu}_2\text{Zn}_{0.5}\text{Sn}_{0.9}\text{Se}_{2.8}\text{S}_{0.3}$  (d)  $\text{Cu}_{2.3}\text{Hg}_{0.7}\text{Ge}_{1.0}\text{Se}_4$  (e)  $\text{Cu}_2\text{HgGeSe}_4$  (f)  $\text{Cu}_2\text{ZnSnS}_4$  nanorods (g)  $\text{Cu}_2\text{CdSnSe}_4$ , (h)  $\text{Cu}_2\text{ZnSnSe}_4$  and (i)  $\text{Cu}_2\text{ZnSnS}_4$  NPs (An inset of a, b, d, e, and g displays a histogram of the matching NPs particles size) [9, 40-44].

## 1. The structure of crystals

The reactivity of cationic precursors varies, making it difficult to stoichiometrically control the generation of many compositional phases by quaternary nanocrystals during the primary phases of the reaction.

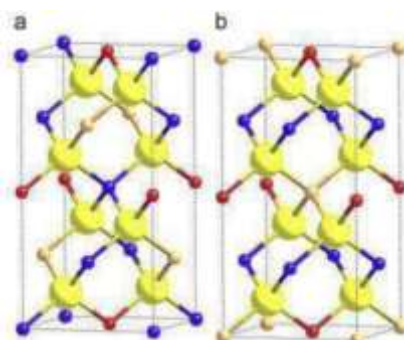


**Figure 6:** (a) The kesterite design, (b) the stannite design (the colors are blue for Cu; orange for Zn; red for Sn; and yellow for Se/S).

Copper zinc tin sulfide (CZTS) and copper zinc tin selenide (CZTSe) are researched as possible alternatives to CIGS in solar cells. Their crystalline structure consists of alternating CuSn and CuZn layers along the c-axis orientation. CZTS and CZTSe are synthesized tetragonal kesterite structures (spatial group I 4; Fig. 6). They exhibit spin around a c-axis and contain pure Cu and SnZn layers in a stannite structure (space group I-42m). The identical scattering ability of the isoelectronic cations  $\text{Cu}^+$  and  $\text{Zn}^{2+}$  makes it difficult to distinguish between them using X-ray diffraction. However, because of the differences between respective neutron scattering wavelengths, a structural investigation using neutron diffraction is possible [45]. According to production methods revealed for various binary and ternary metallic chalcogenide nanoparticles, comparable approaches have recently been discovered for CZTS, CZTSe, and a few more materials. According to Hirai et al. in 1967, the figure in Scheme 7 clearly illustrates the cross-replacement of group IV elements to produce quaternary chalcogenides [46].

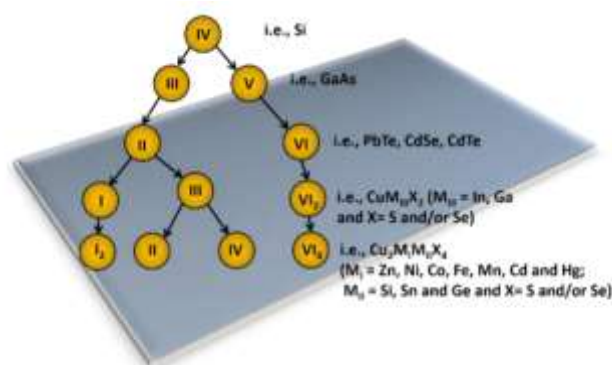


**Figure 7:** Diagrammatic that illustrates how quaternary chalcogenides are formed [46].

The quaternary chalcogenides are known for their versatility in terms of physical attributes, owing to their greater degree of structure and chemical freedom. It has been well-documented that these chalcogenides crystallize within kesterite and stannite crystalline phases, with only minor differences in their formation energies. Specifically, the formation energy is 1.3 meV per atom based on S molecules, while it is 3.3 meV/atom based on Se molecules [47, 48]. Steady-state growth conditions lead to the formation of the kesterite structure, in which a CZTX consists of consecutive Cu-Sn and Cu-Zn cationic layers. Kesterite and stannite have similar characteristics, so they can coexist depending on the synthesis conditions. The c-axis-oriented

stannite structure, which consists of pure copper and tin-zinc layers, is displayed in Fig. 7. A recent discovery includes the wurtzite phase of quaternary chalcogenides. [49–54]. Due to the minor energy difference that results in the disordered thermodynamic orthorhombic phase, the arrangement of having Cu and Zn as cation locations remains similarly susceptible to randomness [1, 55]. Fig. 8 illustrates the crystal phases that quaternary chalcogenides can form. Due to the same scattering energies of isoelectronic  $\text{Cu}^+$  and  $\text{Zn}^{2+}$ , the enormous mass XRD patterns for CZTX, the kesterite and stannite phases, are identical. Even so, because the various crystal phases' neutron scattering wavelengths varied, it was possible to distinguish between them utilizing neutron diffraction technology [45].

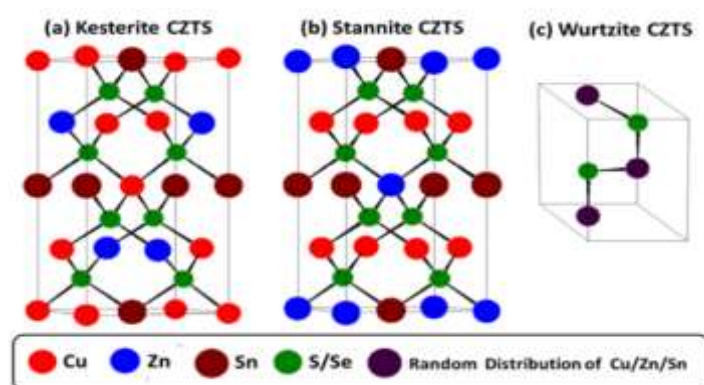


**Figure 8:** The CZTS conventional unit cells, including the crystal construction of (a) kesterite, (b) stannite, and (c) wurtzite [45].

In relation with its bonding properties, crystallite, and electrical conductivity, CZTX is similar to and descended from  $\text{CuMIIX}_2$  (M is In, Ga, while X is S, Se) [56–58]. Therefore, it is thought that the CZTX has a p-type conductivity, which is derived from its prevalent Cu vacancy ( $\text{VCu}$ ), such analogous to how  $\text{CuMIIX}_2$  behaves [31–66]. Nonetheless, Chen et al.'s first-principles calculations for several intrinsic defects and defect complexes in CZTX provide several intriguing findings [47, 31, 59–61, 66]. They proposed that the production energy of a CuZn crystal lattice defect, which predominates over  $\text{VCu}$  a steady-state chemical potential region among some of the numerous defects generated as it relates to the CZTX, including  $\text{VCu}$ ,  $\text{VZn}$ , in addition, to crystal lattice disorder  $\text{CuZn}$ ,  $\text{CuSn}$ , and  $\text{ZnSn}$  flaws, appear to have the lowest value among those formed [59, 49, 67]. The role of electrically neutral defect

complexes for example,  $[Cu-Zn-Zn^+-Cu]$ ,  $[V-Cu-Zn^+-Cu]$  and  $[Zn_2-Sn-2Zn^+-Cu]$  is predicted to be important, energy sources and electronic passivation massive levels within the band gap energy at reducing loss of production [68]. Due to the many acceptor defects having low formation energies, such systems are inherently p-type, making n-type doping extremely challenging and uncommon [31, 60]. Groups IV and VI, as well as Cu(X) element energetic states have a significant impact on the optical characteristics. The valence band orbitals with SP produced via the orbital S of an elements IV group as well as X's 3P orbitals make up the majority of the edge states of the conduction band (CB) in chalcogenides for a quaternary component. Lowering the CB minimal level and splitting are caused by weaker hybridization between these orbitals, which reduces the binding energy. As a result, molecules containing Sn's energy gap are narrower than those containing Ge for the reason that the CB minimal is lower and attributed to hybridization being weaker. Transitions of XP and Cu 3d make up the majority of the valence band (VB) states. Smaller band gaps produced by hybridization of these transitions are relatively weak, which also causes fewer splits and a higher greatest VB. Because of the greater CB maximum caused by the weaker hybridization, materials at sea exhibit narrow band gaps relative to those at S [50, 69]. The figure illustrates various hybridization states used to form VB and CB (Fig. 9) [70].

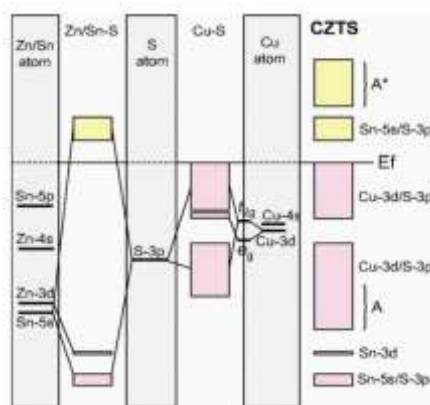


**Figure 9:** Depicts the chemical interactions, intensities of one electron per atom, and CZTS band structure. The hybridization of forming bands at cation-S is noticed, as well as the creation of bonding linear combinations (A), and antibonding linear combinations (A\*). The atomic levels determine the vacuum level alignment. [70].



Defect generation energy in complex semiconductors made of four elements is determined by a theory based on thermodynamics and excess atomic chemical potential. The  $\text{Cu}_2\text{ZnSnX}_4$  (CZTX) as an example, requires a specific chemical potential of Cu, Zn, Sn, and X, achieved by following a specific relation:

$$2\mu_{\text{Cu}} + \mu_{\text{Zn}} + \mu_{\text{Sn}} + 4\mu_{\text{X}} = \Delta H_f(\text{CZTX}) \quad (1)$$

The limited constrained stability of the phase zone having CZTX has a significant impact mostly on the synthesis process., This requires extreme vigilance to prevent the formation of six solid sets, which include :  $\text{Cu}_2\text{SnX}_3$ ,  $\text{ZnX}$ ,  $\text{CoX}$ ,  $\text{Cu}_2\text{X}$ ,  $\text{SnX}$ , and  $\text{Cu}_2\text{X}$  [71].

The values of  $\mu_{\text{Cu}}$ ,  $\mu_{\text{Zn}}$ ,  $\mu_{\text{Sn}}$ , and  $\mu_{\text{X}}$  should be less than zero in order to prevent the formation of FCC (face-centered cubic) structures utilizing pure metal lattices of Copper (Cu), Zinc (Zn), Tin (Sn), and any other metal (X). Additionally, the equation  $\Delta H_f(\text{CZTX}) - \Delta H_f(2\text{CuX}) - \Delta H_f(\text{ZnX}) - \Delta H_f(\text{SnX})$  should be less than zero in order to make CZTX (Copper-Zinc-Tin-X) with a formation enthalpy ( $\Delta H_f$ ) that is lower than the enthalpy of production of  $\text{CuX}$ ,  $\text{ZnX}$ , and  $\text{SnX}$ . To avoid the formation of an alternative structure, the equation  $\Delta H_f(\text{CZTX}) - \Delta H_f(\text{Cu}_2\text{X}) - \Delta H_f(\text{ZnX}) - \Delta H_f(\text{SnX}_2)$  should also be smaller than zero. The synthesis of CZTS phase can be achieved by combining binary compounds  $2\text{CuX} + \text{ZnX} + \text{SnX}$  and  $\text{Cu}_2\text{X} + \text{ZnX} + \text{SnX}_2$  at high temperatures [38, 72, 73, 74-100]. The depicted Fig. 10 CZTS phase diagram for the stable CZTS formation region and parameters to prevent new binary and ternary phases.

## 2. Energy Band Structure.

The lack of understanding of the fundamental composition and crystal structure of solar cell materials makes it challenging to research their electrical and optical properties, as well as their energy bandwidth, state density, doping behavior, and transport properties. For  $\text{Cu}_2\text{ZnSnS}_4$  and  $\text{Cu}_2\text{ZnSnSe}_4$ , numerous theoretical results indicate that the sulfide's band gap is greater than the selenide's [98]. remarkably, a variety of Cu-based quaternary chalcogenide chemical compounds have recently surfaced and are described as having a variety of uses. Examples of these materials are  $\text{Cu}_2\text{MIMIX}_4$ , where  $\text{MI} = \text{Zn, Ni, Co, Fe, Mn, Cd, and Hg}$ ;  $\text{MII} = \text{Si, Sn, and Ge}$ ; and  $\text{X} = \text{S and/or Se}$  [76-81].

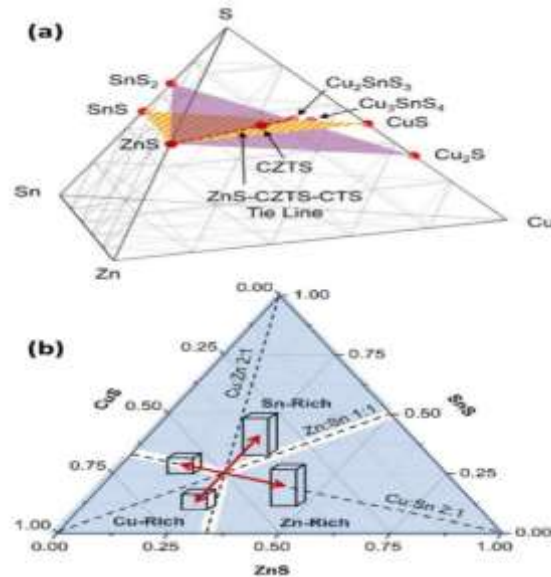


**Figure 10:** (a) A schematic of the observed phases in the CZTS quaternary system. The figure is a schematic of two pseudo-ternary planes intersecting at the ZnS-Cu<sub>2</sub>ZnSnS<sub>4</sub>-Cu<sub>2</sub>SnS<sub>3</sub> tie line. (b) On the pseudo-ternary diagram, the boundaries of the Cu-, Sn-, and Zn-rich zones are established by the Cu/Sn = 2; Cu/Zn = 2; and Zn/Sn = 1 tie lines. Lastly, the text describes the trends in the crystalline structures of the Cu<sub>2</sub>SnS<sub>3</sub> on films produced at 325 °C, which coexists with CZTS and ZnS within these various compositional zones. [71].

### 3. Preparation Methods

#### 3.1 Electrochemical Deposition Method

To decrease the number of cations in a liquid substance or product, one effective strategy is using electrochemical precipitation or hot-plunge liquid at the cathode by utilizing the power of the external circuit. In the 1970s, people began experimenting with semiconductor material electrochemical explanations [82, 83]. Electrodeposition is presently utilized to produce solar cells, such as CIGS solar cells manufactured by France's CISEL [84] and CdTe cells manufactured by BP plc [85]. However, employing thiourea as an alternative for CdS in the electrodeposition process has proven difficult in identifying areas of strength for this source [86]. CZTS, a material used in solar cells, was deposited at Bath University in Britain in 2008 utilizing the procedure of covering and constructing Cu/Sn/Zn, resulting in a conversion



efficiency of 0.8% [87-88]. In 2010, an improved development obtained a 3.2% conversion efficiency employing a natural environment of powder S and 10% H<sub>2</sub> in an N<sub>2</sub> conveyance gas prepared for two hours at 575°C [89]. In 2009, Nagaoka University of Technology used electrodeposition on Cu/Sn/Zn cover and in this way kept up with it for two hours in the carrier gas with sulfur powder at 600 °C to achieve a change limit of 0.98% percent. To deal with the substrate's adherence, they added a Pb layer deposited onto a surface Mo before electrodeposition [90]. They succeeded in obtaining solar-powered devices with a 3.16% change limit percent. Following two hours of treatment at 600 °C in a sulfur-containing carrier gas, CuZnSn was co-deposited in a single-process blend [91].

Ennaoui in Germany and HZB developed a CZTS photovoltaic with a photovoltaic efficiency of 3.4% around the same time. They used a one-time co-deposition process comprising 30mm Sn<sup>2+</sup>, 3mm Zn<sup>2+</sup>, and 3mm Cu<sup>2+</sup> to make CZTS films employing Cu of it with the CuxS in the KCN build result in scratching with 3.5% thickness. Later, they planned it after 10 minutes of light treatment, and its sensitivity was 3.6% [8, 92].

In 2012, IBM devised a method for generating CuZnSn alloy by heating a copper, zinc, and tin cover in N<sub>2</sub> for 30 minutes at 350°C. The cover was then heated for 12 minutes at 585°C in an N<sub>2</sub> atmosphere containing sulfur. CdS and ZnO were combined to produce CZTS solar cells with a capacity of 7.3%. [93].

Utilizing a systematic Slow Ionic Layer Adsorption and Reaction (SILAR) mechanism on an SLG glass substrate, Shinde et al. have recently found a new technique for producing CZTS films. To make CZTS thin films, the substrate is immersed in a 1:1:1 ratio of cationic precursor solutions (0.1M CuSO<sub>4</sub>, 0.05M ZnSO<sub>4</sub>, 0.05M SnSO<sub>4</sub>) and anionic precursor solution (0.2M thioacetamide). The films were then heated for four hours at 400°C. This technique yielded a low-cost CZTS film with a photoluminescence sensitivity of 0.12%, which is appropriate for use in solar cells that use photovoltaic [94, 95]. Miao et al. used an electrochemical technique to develop film solar energy cells, which were then post-sulphurized at 500°C and 550°C. The crystallinity of the models improved as the sulfurization temperature increased, revealing that the CFTS small films contain a stannite structure. Raman and X-ray photoelectron spectroscopy



were used to identify the constituent molecules as copper (I), iron (II), tin (IV), and sulfur (II). Band-broadening enhancements of 1.35 eV and 1.40 eV were seen after sulfurization treatments at 500°C and 550°C, respectively [96]. The application of a thin coating on a substrate at low temperatures is recognized when employing the electrochemical deposition process since it doesn't add any additional thermal strain. It is also guaranteed by this procedure that the film may be consistently placed on soft and complicated surfaces and adhere well to the substrate. The film is a flexible alternative for a range of applications because its thickness, structure, and porosity can all be carefully regulated. The final film has improved material characteristics and is cost-effective.

### 3.2. Mix of nanoparticles by substance and genuine strategies.

Various practical and feasible procedures are employed in the manufacturing of CFTS thin films. Chemical spray deposition and spray pyrolysis systems are two non-vacuum-based technologies used to create CFTS thin films. Vacuum-based technologies, such as sputtering and vacuum co-deposition, are also utilized to create inexpensive and high-quality CFTS thin films for solar cells. The CFTS thin film experiment has two stages: covering the substrate and hardening the material. The first stage is critical for creating thin and homogeneous films on substrates such as Mo-coated glass, while the second stage enhances grain structure and orientation. This section describes easy and efficient approaches for producing miniaturized CFTS thin films.

#### 3.2.1 Nanoparticles by substance structures

New materials technologies without a vacuum are appealing due to their speed, cost, and low-temperature requirements. It may be less costly to get Copper Ferrite Tin Sulfide as a result of these integrated methods. Adsorption, surface dispersion, reaction, production, and improvement are among several of the many phases that reactant particles can be effectively transported through by the simple chemical process known as film distillation [111]. Through a relatively easy chemical method, Guan et al. developed Copper Ferrite Tin Sulfide (CFTS) thin films. The CuSnS film was treated with sulfur and coated with FeS<sub>2</sub> to form CFTS. Cu<sub>2</sub>S



and SnS<sub>2</sub> reacted to form Cu<sub>2</sub>SnS<sub>3</sub>, which in turn reacted with FeS<sub>2</sub> to produce Cu<sub>2</sub>FeSnS<sub>4</sub>. Before the start of treatment, SEM images showed significant micro-aggregates; nevertheless, the film surface developed into a nanorod-like structure following 500 °C treatment. The bandgap energy of the first film decreased as a result of the CFTS treatment [97].

### 3.2.2. Nanoparticles by compound frameworks by ensured structures

Utilizing post-sulfurization and RF magnetization, Meng et al. produced inexpensive CFTS films on glass substrates coated with Mo. Blending materials with high iron content and low copper content improved solar energy conversion efficiency. Photovoltaic energy reliant on CFTS was obtained by sputtering filming an annealed Cu-Fe-Sn in an atmosphere containing precursor sulfur powder. To develop a CFTS-dependent solar cell, they eventually used glass, CFTS, MO, CdS, AZO, and I-ZnO. (J<sub>sc</sub>) of 2.5 mA/cm<sup>2</sup>, (V<sub>oc</sub>) of around 110 mV, and a fill factor (FF) of roughly 26.3% were the measurements of the solar cells [98].

### 3.3. The Spraying of Chemical Pyrolysis

During the spray pyrolysis process, a substrate's surface is heated to around 600°C. Next, one or more metal salt solutions are sprayed over the substrate surface. Pyrolysis caused by the high temperature spray coating will leave a thin film on the substrate's surface. The substrate temperature affects the composition and function of spray pyrolysis thin films. If the substrate temperature is too low, the film's crystallization quality decreases. Maintaining a temperature between 500°C and 650°C can improve the optical properties of the CZTS thin film. Kamoun vulcanized CuCl<sub>2</sub>, ZnCl<sub>2</sub>, and SnCl<sub>2</sub> by spray pyrolysis in a SC(NH<sub>2</sub>)<sub>2</sub> solution. After reacting for an hour at 340°C (the substrate temperature), the materials were annealed at 550°C for 120 minutes. This led to the formation of 1.5 eV band gap CZTS thin films. The experimental technique is simple to implement because it does not require a vacuum or gas protection apparatus. Thin-film materials are low-cost and function well [99].

### 3.4. Solvo-hydrothermal nanoparticle production

Both solvothermal and hydrothermal processes are well known to synthesize nanostructures that are advantageous for the environment [100]. The best method for producing fine



nanoparticles of huge, higher-quality crystals with an exact control over the product's composition is the solvothermal process. The single distinction between hydrothermal and solvothermal reactions is the precursor solution [101]. Gui et al. used a hydrothermal method at a low temperature to manufacture flaky-shaped CFTS nanostructures. Because longer treatment periods have minimal influence on final product quantities or crystallinity, the reaction temperature is essential. Lower than 220 °C cannot be Cu<sub>2</sub>FeSnS<sub>4</sub> and Cu<sub>2</sub>CoSnS<sub>4</sub> prepared [21]. A hydrothermal reaction technique was created by An et al. to produce Cu- and Ag-based nanocrystallites with polydispersed nanoparticles that had a diameter of 10–20 nm [102].

### 3.5. Sol-Gel Method

Sol-gel is a material chemistry formed by hydrolyzing and polycondensing metal compounds, such as salts or alkoxides, in particular solvents. This method can be done by dipping or spin-coating. Once gelatinized, the Sol-gel is heated to form either amorphous or crystalline sheets. To manufacture Sol-gel, a precursor solution containing the required ions is prepared and spin-coated onto a glass surface, forming a thin film. Finally, the obtained thin films are annealed at the controlling environmental conditions. Tanaka et al. at Nagaoka University of Technology developed a sol-gel gelatin in 2007 by combining cupric acetate, zinc acetate, and tin chloride. They used dimethyl alcohol as the solvent and ethanolamine as the stabilizer to coat the gel on Mo glass. Spin coating had to be repeated five times to achieve the desired thickness. The gel was spin-coated Mo glass after a five-minute burning in the air at 300°C and an hour of annealing at 500°C in an N<sub>2</sub> gas atmosphere containing 5% H<sub>2</sub>S. They were eventually able to improve the components and crystallinity of the CZTS thin film [103]. Spin-coating and regularly drying the sol resulted in a CZTS film with 1.01% efficiency in 2009 [6]. Efficiency increased to 2.03% in 2011 because of enhanced film components [104]. The method described here uses simple equipment and requires no vacuum to provide a complete thin film overlay on a variety of substrates. Quantitative doping allows for the production of homogeneous multicomponent oxide films with varying compositions and microstructures. However, there are certain difficulties, such as longer manufacturing times for some organic raw materials and



the development of micro-gel pores in the gelatin, which allows gas and organics to escape during drying. By using a sol-gel method and dip-coating deposition of copper, cobalt, tin, and sulfur, Ziti et al. created  $\text{Cu}_2\text{CoSnS}_4$  sorbents. They evaluated and examined the impact of annealing temperature (280°C to 340°C) on the optical, electrical, structural, and morphological characteristics of the material in the absence of sulfur. The band gap decreased from 1.72 to 1.5 eV upon annealing [105].

### 3.6. Nanoparticles by microwave method

It has been discovered that using microwave-assisted technology produces better, more reliable, high-purity, and size-adjustable results than common synthesis techniques. It is also more economical, time-efficient, and not harmful to the environment [106]. Microwaves can create nanoparticles. Using this method, Guan and his colleagues produced  $\text{Cu}_2\text{CdSnS}_4$  (CCTS) nanoparticles. Following their production, the CCTS nanoparticles were examined utilizing a range of methods, including as UV-Vis-NIR absorbance spectra, X-ray diffraction, EDS, SEM, and TEM. The spherical shape and respectable bandgap ( $E_g = 1.26$  eV) of the CCTS nanoparticles led the researchers to conclude that they would be useful as absorber layers for thin-film solar cells [107].

## 4. Quaternary Chalcogenide Applications

### 4.1. Applications of Photovoltaic

The effectiveness, crystallization, and layer thickness of the materials that are used for manufacturing and constructing solar cells all influence a PV solar cell system's efficiency.

$$\eta = (P_{max}/E * A_c) * 100$$

The information below describes the several elements that influence solar panel efficiency. E (incoming radiation flux in  $\text{Wm}^{-2}$ );  $A_c$  (collector area in square meters);  $V_{oc}$  (open circuit voltage in volts);  $J_{sc}$  (short circuit current density); and FF (fill factor),  $P_{max}$  is the maximum power output (in watts). Many binary chalcogenides, such as CdS, CdSe, PbSe, GaAs,  $\text{Cu}_2\text{S}$ , and ternary  $\text{CuMIIIX}_2$ , have seen significant improvements in solar efficiency [108–120].



However, these chalcogenides have the potential to be unstable and contain hazardous (Pb, As, and Cd) and costly (Ga, In) elements, posing a considerable danger [121–125]. Lead perovskite elements have achieved record effectiveness of 22.1%; however, their Pb-based structure is challenging [122]. While avoiding operational instability, quaternary chalcogenides, in particular kesterite, have the potential to achieve high solar efficiencies comparable to commercial thin-film PV systems or hybrid perovskites. Straight band gaps and optical absorbance values greater than  $10^4 \text{ cm}^{-1}$  are characteristics of Cu-based quaternary chalcogenides [126]. Their band gap energies are in the red end of the solar spectrum, therefore long-term excitation does not affect them [127-129]. Because of its band gap adjustability and optical qualities [130–137], CZTX is a viable alternative for PV applications. Nevertheless [138,139], because of their high defect density and compositional inhomogeneities, quaternary chalcogenide-based solar cells perform poorly and have a low open-circuit voltage ( $V_{oc}$ ). Even with their advantages, several quaternary chalcogenides only yield limited PV efficiencies [160,141-143]. According to photon balance calculations, the maximum efficiency of CZTS and CZTSe thin film solar cells, respectively, is 32.4% and 31.4% [139, 140]. Most recently, advances have proved the use of quaternary chalcogenide thin-film and nanocrystal ink for solar technologies, as illustrated in Figure 11, which illustrates the extraction of both charge capacities and losses. Table 1 illustrates the various methods utilized to create quaternary chalcogenide nanocrystals.

#### 4.2. Troubles and future perspectives

Using both vacuum and non-vacuum techniques, a study examined the development of CFTS-based solar cells by incorporating CFTS material into nanoparticles and thin film structures. Vacuum-based methods, such as sputtering and PLD, can increase the efficiency of solar conversion. Solvothermal systems, microwaves, and hot implantation are examples of non-vacuum techniques. The technique for connecting sunlight to a cell's device using a nanoparticle combination consists of three steps: joining the nanoparticles, coating the substrate with nanoparticle-based ink, and setting. To improve CFTS-based solar cells, monodisperse nanoparticles with excellent optoelectric properties must be regulated in size and shape. When combining CFTS nanoparticles, the solvent used in each reaction step must be carefully chosen.

Instead of expensive and harmful solvents, eco-friendly ones should be utilized when producing CFTS nanoparticles. For dealing with difficulties such as inconsistent grain formation and volume reduction, a variety of film coating processes can be used to provide a uniform protecting layer. The first step in building a solar cell is to manage the sulfur-rich air environment. Annealing high temperatures can cause structural flaws in the barrier layer, lowering the performance of TFSCs. High-temperature laying out also causes the creation of a thick and tough MoS<sub>2</sub> layer at the CFTS/Mo interacting with each other. Recently, a CIGS-based cell achieved a 22.6% limit [121]. Compared to CZTS and CZTSSe-based solar cells, which exhibit efficiencies of 9.5% and 10.8%, respectively, CFTS-based solar cells are less efficient [162, 163]. There is little research on CFTS in thin-film solar cells. It is essential to continually track the crystallization of the barrier layers inhibiting CFTS. For solar cell applications, CFTS material is still a good choice in spite of these difficulties.

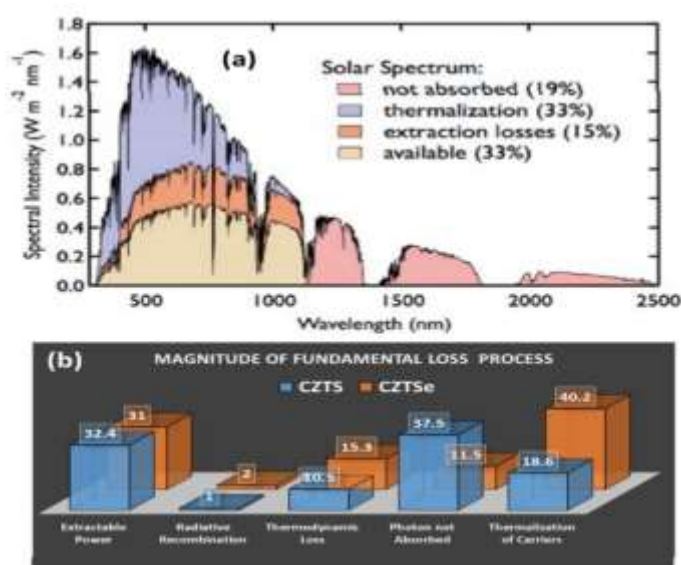


**Figure 11:** (a) illustrates the solar radiation spectrum and the solar radiation available for photovoltaic applications in addition to different losses. (b) Illustrates the CZTS and CZTSe's fundamental loss mechanism, which was established by meticulous balancing calculations.

$V_{oc} = 1.21$  V;  $J_{sc} = 29.6$  mAcm<sup>-2</sup>; FF = 89.9%; and 32.4% efficiency are the ideal performance values for CZTS.  $V_{oc} = 0.71$  V;  $J_{sc} = 51.4$  mAcm<sup>-2</sup>; FF = 84.8%; and 31.0% efficiency are the ideal values for CZTSe [140].



**Table 1:** Methods of substance blend of quaternary chalcogenide nanocrystals.

COMPOUND NAME	METHOD	CRYSTAL STRUCTURE	BAND GAB (EV)	REFERENCES
Cu <sub>2</sub> CoSnS <sub>4</sub>	Chemical spray pyrolysis Sol-Gel Sol-Gel deposited by vacuum thermal evaporation on heated substrates Chemical spray pyrolysis produced via co-electrodeposition of precursors for Cu, Co, S, and S on a molybdenum substrate.	Stannite	1.42 –	[141]
		Stannite	1.79	[142]
		Stannite	1.45	[143]
			1.5-1.72	[144]
			1.40-	[145]
		Stannite	1.43	[146]
			1.52-1.56	
			1.4-1.5	
Cu <sub>2</sub> CdSnS <sub>4</sub>	Chemical spray pyrolysis  deposited by ultrasonic spray method at various substrate temperatures  CdSn(OH) <sub>6</sub> prepared by co-precipitation method as the precursor	Stannite	1.39-1.5	[147]
			1.37	[148]
				[149]
Cu <sub>2</sub> FeSnS <sub>4</sub>	the co-electrochemical deposition	stannite	1.1-1.55	[150]
Cu <sub>2</sub> FeSnS <sub>4</sub>	chemical bath deposition process Chemical spray pyrolysis chemical pyrolysis technique	Kesterite	1.41-1.19	[151]
		Stannite	1-1.5	[152]
		Stannite	1.77-1.92	[153]
Cu <sub>2</sub> ZnSnS <sub>4</sub>	Chemical bath deposition (CBD) is used on soda-lime glass substrates with magnetron sputtering (MS) and pulsed laser deposition (PLD). Via the SILAR technique with various dipping periods and deposited over the conducting and non-conducting surfaces.		1.40	[154]
				[155]
		wurtzite and kesterite	1.46-1.82	[156]
		Kesterite		[157]
			1.62	
Cu <sub>2</sub> NiSnS <sub>4</sub>	Chemical pyrolysis technique. sol-gel	cubic	1.57-1.82	[158]
			1.2-1.7	[159]
Cu <sub>2</sub> CrSnS <sub>4</sub>	Solvothermal	Stannite	1.35-1.54	[160]
Ag <sub>2</sub> ZnSnS <sub>4</sub>	chemical spray pyrolysis	Stannite	2-2.08	[161]



## Conclusions

Materials that were formerly plentiful and inexpensive are now exceedingly expensive and undesirable for the ecosystem due to the growing demand for materials utilized in numerous and multifunctional applications. As a result, the quaternary chalcogenides of I2-II-IV-VI4 family previously used in photovoltaic applications have piqued the curiosity of many researchers. With regard to the morphology, chemical stoichiometric, and composition of the material, these quaternary materials offer a wide range of options for achieving unique features. These quaternary chalcogenides, which are classed as semiconductors, contain a number of different compounds. The functions and properties of commonly used compounds like  $\text{Cu}_2\text{ZnSnS/Se}_4$ ,  $\text{Cu}_2\text{FeSnS}_4$ ,  $\text{Cu}_2\text{MnSnS}_4$ ,  $\text{Cu}_2\text{NiSnS}_4$ , and  $\text{Cu}_2\text{CoSnS}_4$  are highlighted in this study because they excite the interest of researchers. In addition to the finding of a newly devised crystal structure represented by the wurtzite phase, the quaternary chalcogenides were found to have a common crystal structure that includes the Kesterite and stannite phases. The optical energy gap in these quaternary compounds is smaller than that of the two- and three-compounds because of the relatively small energy gap in the quaternary case and the fact that the band gap of quaternary compounds containing sulfide is larger than that of quaternary compounds containing selenium. Most such compounds revealed a wide range of applications, providing a strong motivation to further investigate these materials and learn more about their applications.

## References

1. H.Jiang, P.Dai, Z.Feng, W.Fan and J.Zhan, Phase Selective Synthesis of Metastable Orthorhombic  $\text{Cu}_2\text{ZnSnS}_4$ . *Journal of Materials Chemistry* ,Vol. 22 ,pp. 7502-7506, (2012).
2. W. Hsu, C. M. Sutter-Fella, M. Hettick, L. Cheng, S. Chan, Y. Chen, Y. Zeng, M. Zheng, H. Wang, C. Chiang, and A. Javey, Electron-Selective  $\text{TiO}_2$  Contact for Cu (In, Ga)  $\text{Se}_2$  Solar Cells. *Scientific reports*, Vol. 5, pp. 1-7, (2015).
3. Q. Guo, G. M. Ford, W. C. Yang, B. C. Walker, E. A. Stach, H. W. Hillhouse and R. Agrawal, Fabrication of 7.2% Efficient CZTSSe Solar Cells Using CZTS Nanocrystals, *J. Am. Chem. Soc* ,Vol. 132, pp. 17384–17386, (2010).



4. M. Nakamura, K. Yamaguchi and Y. Kimoto, Cd-Free Cu(In,Ga)(Se,S)<sub>2</sub> Thin-Film Solar Cell with Record Efficiency of 23.35%. *IEEE J. Photovolt*, Vol. 9, pp. 1863–1867, (2019).
5. H. Katagiri, K. Jimbo, W. S. Maw, K. Oishi, M. Yamazaki, H. Arak and A. Takeuchi, Development of CZTS-Based thin Film Solar Cells, *Thin Solid Films* ,Vol. 517 ,pp. 2455-2460, (2009).
6. K. Tanaka, M. Oonuki, N. Moritake and H. Uchiki, Cu<sub>2</sub>ZnSnS<sub>4</sub> thin film solar cells prepared by Non-Vacuum Processing. *Solar Energy Materials and Solar Cell*, Vol. 93, pp. 583-587, (2009).
7. A. Weber, S. Schmidt, D. Abou-Ras, P. S. Bischoff, I. Denks, R. Mainz and H. W. Schock, Texture Inheritance in thin-Film Growth of Cu<sub>2</sub>ZnSnS<sub>4</sub>. *Applied Physics Letters* ,Vol. 95 ,pp. 041904, (2009).
8. Q. Guo, H. W. Hillhouse and R. Agrawal, Synthesis of Cu<sub>2</sub>ZnSnS<sub>4</sub> nanocrystal ink and its use for Solar Cells *Journal of the American Chemical Society* ,Vol. 131 ,pp. 11672-11673, (2009).
9. C. Steinhagen, M. G. Panthani, V. Akhavan, B. Goodfellow, B. Koo and B. A. Korgel, Synthesis of Cu<sub>2</sub>ZnSnS<sub>4</sub> Nanocrystals for Use in low-cost Photovoltaics. *Journal of the American Chemical Society* ,Vol. 131 ,pp. 12554-12555, (2009).
10. A. Shavel, J. Arbio and A. Cabot, Synthesis of Quaternary Chalcogenide Nanocrystals: Stannite Cu<sub>2</sub>Zn<sub>x</sub>Sn<sub>y</sub>Se<sub>1+x+2y</sub>. *Journal of the American Chemical Society* ,Vol. 132 , pp. 4514-4515, (2010).
11. S. Ahn, S. Jung, J. Gwak, A. Cho, K. Shin, K. Yoon, D. Park, H. Cheong, and J. Ho. Yun, Determination of band gap energy (E<sub>g</sub>) of Cu<sub>2</sub>ZnSnSe<sub>4</sub> thin films: on the discrepancies of reported band gap values. *Applied Physics Letters* ,Vol. 97 ,pp. 021905, (2010).
12. T. K. Todorov, K. B. Reuter, and D. B. Mitzi, High-efficiency solar cell with earth-abundant liquid-processed absorber. *Advanced materials* ,Vol. 22 ,pp. 156-159, (2010).



13. P. Balaza, M. Balaza, A. Zorkovskaa, I. Škorvánekb, Z. Bujnakovaa and J. Trajic, Kinetics of solid-state synthesis of quaternary  $\text{Cu}_2\text{FeSnS}_4$  (stannite) nanocrystals for solar energy applications. *Acta Phys* ,Vol. 131 ,pp. 1153-1155, (2017).
14. H. Oueslati, M. B. Rabeh and M. Kanzari, Growth and characterization of the evaporated quaternary absorber  $\text{Cu}_2\text{FeSnS}_4$  for solar cell applications. *Journal of Electronic Materials* ,Vol. 47, p. 3577-3584, (2018).
15. S. Siebentritt. Why are kesterite solar cells not 20% efficient? *Thin solid films*, Vol. 535 ,pp. 1-4, (2013).
16. X. Wang, X. Gu, H. Guan, and F. Yu, Flower-like  $\text{Cu}_2\text{MnSnS}_4$  particles synthesized via microwave irradiation method. *Chalcogenide Lett* ,Vol. 12, 99-103, (2015).
17. L. Nie, J. Yang, D. Yang and S. Liu, Effect of substrate temperature on growth and properties of  $\text{Cu}_2\text{MnSnS}_4$  thin films prepared by chemical spray pyrolysis. *Journal of Materials Science: Materials in Electronics* ,Vol. 30 ,pp. 3760-3766, (2019).
18. A. Lunhong, and Jing Jiang. Hierarchical porous quaternary Cu–Fe–Sn–S hollow chain microspheres: rapid microwave nonaqueous synthesis, growth mechanism, and their efficient removal of organic dye pollutant in water. *Journal of Materials Chemistry* , Vol. 22 ,pp. 20586-20592, (2012).
19. L. Ai and J. Jiang, Self-sacrificial templating synthesis of porous quaternary Cu–Fe–Sn–S semiconductor nanotubes via microwave irradiation. *Nanotechnology*, vol. 23.49, pp. 495601 ,(2012).
20. C. Yan, C. Huang, J. Yang, F. Liu, J. Liu, Y. Lai, J. Li and Y. Liu, Synthesis and characterizations of quaternary  $\text{Cu}_2\text{FeSnS}_4$  nanocrystals. *Chemical Communications* ,Vol. 48.20, pp. 2603-2605, (2012).
21. Z. Gui, R. Fan, X. Chen, Y. Hu, Z. Wang, A new colloidal precursor cooperative conversion route to nanocrystalline quaternary copper sulfide. *Materials research bulletin*, Vol. 39.2 ,pp. 237-241, (2004).
22. X. Jiang, W. Xu, R. Tan, W. Song, J. Chen, Solvothermal synthesis of highly crystallized quaternary chalcogenide  $\text{Cu}_2\text{FeSnS}_4$  particles. *Materials Letters* ,vol. 102 , pp. 39-42, (2013).



23. X. Meng, H. Deng, J. He, L. Sun, P. Yang, J. Chu, Synthesis, structure, optics and electrical properties of  $\text{Cu}_2\text{FeSnS}_4$  thin film by sputtering metallic precursor combined with rapid thermal annealing sulfurization process. *Materials Letters* ,Vol. 151 ,pp. 61-63, (2015).
24. R. Prabhakar, N. H. Loc, M. H. Kumar, P.P. Boix, S. Juan, R. A. John, S. K. Batabyal, and L.H. Wong, Facile water-based spray pyrolysis of earth-abundant  $\text{Cu}_2\text{FeSnS}_4$  thin films as an efficient counter electrode in dye-sensitized solar cells. *ACS applied materials & interfaces* ,Vol. 6.20 ,pp. 17661-17667, (2014).
25. W. Wang, H. Shen, H. Yao, J. Li, Preparation and properties of  $\text{Cu}_2\text{FeSnS}_4$  nanocrystals by ultrasound-assisted microwave irradiation. *Materials Letters* ,Vol. 125 , pp. 183-186, (2014).
26. J. Zhou, Z. Ye, Y. Wang, Q. Yi, and J. Wen, Solar cell material  $\text{Cu}_2\text{FeSnS}_4$  nanoparticles synthesized via a facile liquid reflux method. *Materials letters* ,Vol.140 , pp. 119-122, (2015).
27. L. Chen, H. Deng, J. Tao, W. Zhou, L. Sun, F. Yue, P. Yang, and J. Chu, Influence of annealing temperature on structural and optical properties of  $\text{Cu}_2\text{MnSnS}_4$  thin films fabricated by sol-gel technique. *Journal of Alloys and Compounds* ,Vol. 640 ,pp. 23-28, (2015).
28. R. R. Prabhakar, S. Zhenghua, Z. Xin, T. Baikie, L. S. Woei, S. Shukla, S. K. Batabyal, O. Gunawan, and L. H. Wong, Photovoltaic effect in earth abundant solution processed  $\text{Cu}_2\text{MnSnS}_4$  and  $\text{Cu}_2\text{MnSn}(\text{S}, \text{Se})_4$  thin films. *Solar Energy Materials and Solar Cells* , Vol. 157 ,pp. 867-873, (2016).
29. X. Yan, E. Michael, S. Komarneni, J. R. Brownson and Z. Yan, Microwave-Hydrothermal/Solvothermal Synthesis of Kesterite, an Emerging Photovoltaic Material. *Ceramics International* ,Vol. 40.1 ,pp. 1985-1992, (2014).
30. Y. Liu, J. Xu, Z. Ni, G. Fang and W. Tao, One-Step Sonochemical Synthesis Route Towards Kesterite  $\text{Cu}_2\text{ZnSnS}_4$  Nanoparticles. *Journal of Alloys and Compounds* , Vol. 630 ,pp. 23-28, (2015).



31. S. Chen, X. Gong, A. Walsh and S. H. Wei, Electronic Structure and Stability of Quaternary Chalcogenide Semiconductors Derived From Cation Cross-Substitution of II-VI and I-III-VI<sub>2</sub> Compounds. *Physical Review B* ,vol. 79 ,pp. 165211, (2009).
32. Z. Li, J. W. Ho, K. K. Lee, X. Zeng, T. Zang, L. H. Wong and Y. M. Lam, Environmentally Friendly Solution Route to Kesterite Cu<sub>2</sub>ZnSn(S, Se)<sub>4</sub> thin Films for Solar cell Applications. *RSC Advances* ,Vol. 4.51 ,pp. 26888-26894, (2014).
33. K. Sun, Z. Su, C. Yan, F. Liu, H. Cui, L. Jiang , Y. Shen, X. Hao and Y. Liu, Flexible Cu<sub>2</sub>ZnSnS<sub>4</sub> Solar Cells Based on Successive Ionic Layer Adsorption and Reaction Method. *RSC Advances* ,Vol. 4.34 ,pp. 17703-17708, (2014).
34. T. J. Huang, X. Yin, C. Tang, G. Qi and H. Gong, A low-cost, ligand Exchange-Free Strategy to Synthesize Large-Grained Cu<sub>2</sub>ZnSnS<sub>4</sub> thin-Films without a Fine-Grain Underlayer from Nanocrystals. *Journal of Materials Chemistry A* ,Vol. 3.34 ,pp. 17788-17796, (2015).
35. N. Yu, R. Zhong, W. Zhong, X. Chen, J. Luo, X. Gu, X. Hu, L. Zhong, J. Hu and Z. Chen Synthesis of Cu<sub>2</sub>ZnSnS<sub>4</sub> Film by Air-Stable Molecular-Precursor ink for Constructing thin Film Solar Cells. *RSC advances* ,Vol. 4.68 ,pp. 36046-36052, (2014).
36. N. S. Arul, D. Y. Yun, D.U. Lee and T. W. Kim, Strong Quantum Confinement Effects in Kesterite Cu<sub>2</sub>ZnSnS<sub>4</sub> Nanospheres for Organic Optoelectronic Cells. *Nanoscale* , Vol. 5.23 ,pp. 11940-11943, (2013).
37. A. P. Alivisatos, Semiconductor Clusters, Nanocrystals, and Quantum Dots. *Science* , Vol. 271, pp. 933-937, (1996).
38. C. S. Riha, B. A. Parkinson, and A. L. Prieto, Solution-Based Synthesis and Characterization of Cu<sub>2</sub>ZnSnS<sub>4</sub> Nanocrystals. *Journal of the American Chemical Society* ,Vol. 131 ,pp. 12054-12055, (2009).
39. M. Ibanez, D. Cadavid, R. Zamani, N. G. Ctello, V. I. Roca, W. Li, A. Fairbrother, J. D. Prades, A. Shavel, J. Arbio, A. P. Rodriguez, J. R. Morante and A. Cabot, Composition Control and Thermoelectric Properties of Quaternary Chalcogenide Nanocrystals: the Case of Stannite Cu<sub>2</sub>CdSnSe<sub>4</sub>. *Chemistry of Materials* ,Vol. 24 ,pp. 562-570, (2012).



40. W. Li, M. Ibanez, R. R. Zamani, N.G. Castello, S. Crosse, D. Cadavid, J. D. Prades, J. Arbiol and A. Cabot, Cu<sub>2</sub>HgSnSe<sub>4</sub> Nanoparticles: Synthesis and Thermoelectric Properties. *Cryst Eng Comm* ,Vol. 15 ,pp. 8966-8971, (2013).
41. W. Li, M. Ibanez, D. Cadavid, R. R. Zamani, J. R. Garcia, S. Gorse, J. R. Morante, J. Arbiol and A. Cabot, Colloidal Synthesis and Functional Properties of Quaternary Cu-Based Semiconductors: Cu<sub>2</sub>HgGeSe<sub>4</sub>. *Journal of nanoparticle research* ,Vol. 16 ,pp. 1-6, (2014).
42. F. J. Fan, L.Wu, M. Gong, S. Y. Chen, G. Y. Liu, H. W. Liang, Y. X. Wang and S. Hong Yu, Linearly Arranged Polytropic CZTSSe Nanocrystals. *Scientific reports* ,Vol. 2 ,pp. 1-6 ,(2012).
43. K. Wei and G. S. Nolas, Synthesis and Characterization of Nanostructured Stannite Cu<sub>2</sub>ZnSnSe<sub>4</sub> and Ag<sub>2</sub>ZnSnSe<sub>4</sub> for Thermoelectric Applications. *ACS applied materials & interfaces* ,Vol. 7 ,pp. 9752-9757, (2015).
44. J. J. Wang, P. Liu and K. M. Ryan, A Facile Phosphine-Free Colloidal Synthesis of Cu<sub>2</sub>SnS<sub>3</sub> and Cu<sub>2</sub>ZnSnS<sub>4</sub> Nanorods with a Controllable Aspect Ratio. *Chemical Communications* ,Vol. 51 ,pp. 13810-13813, (2015).
45. S. Schorr, The Crystal Structure of Kesterite Type Compounds: A Neutron and X-ray Diffraction Study. *Solar Energy Materials and Solar Cells* ,Vol. 95 ,pp. 1482-1488, (2011).
46. T. Hirai, K. Kurata, and Y. Takeda, Derivation of New Semiconducting Compounds by Cross Substitution for Group IV Semiconductors, and their Semiconducting and Thermal Properties. *Solid-State Electronics* ,Vol. 10, pp. 975-981, (1967).
47. S. Chen, X. G. Gong, A. Walsh, and S. Wei, Crystal and electronic band structure of Cu<sub>2</sub>ZnSnX<sub>4</sub> (X=S and Se) photovoltaic absorbers: First-principles insights *Applied Physics Letters*, vol. 94 ,pp. 041903, (2009).
48. C. Persson, Electronic and Optical Properties of Cu<sub>2</sub>ZnSnS<sub>4</sub> and Cu<sub>2</sub>ZnSnSe<sub>4</sub>. *Journal of Applied Physics* ,Vol. 107 ,pp. 053710, (2010) .



49. X. Lu, Z. Zhuang, O. Peng and Y. Li, Wurtzite  $\text{Cu}_2\text{ZnSnS}_4$  Nanocrystals: a Novel Quaternary Semiconductor. *Chemical Communications* ,Vol. 47 ,pp. 3141-3143, (2011).
50. M. Li, W. H. Zhou, J. Guo, Y. Lizhou, Z. L. Hou, J. Z. Jizhou, Z. L. Du and S. X. Wu, Synthesis of pure Metastable Wurtzite CZTS Nanocrystals by Facile one-Pot Method. *The Journal of Physical Chemistry C* ,Vol. 116 ,pp. 26507-26516, (2012).
51. A. Singh, H. Geaney, F. Laffir and K. M. Ryan, Colloidal Synthesis of Wurtzite  $\text{Cu}_2\text{ZnSnS}_4$  Nanorods and Their Perpendicular Assembly. *Journal of the American Chemical Society* ,Vol. 134 ,pp. 2910-2913, (2012).
52. C. C. Kang, H. F. Chen, T. C. Yu and T. C. Lin, Aqueous Synthesis of Wurtzite  $\text{Cu}_2\text{ZnSnS}_4$  Nanocrystals. *Materials Letters* ,Vol. 96 ,pp. 24-26, (2013).
53. X. Zhang, N. Bao, B. Lin and A. Gupta, Colloidal Synthesis of Wurtzite  $\text{Cu}_2\text{CoSnS}_4$  Nanocrystals and the Photoresponse of Spray-Deposited thin Films. *Nanotechnology* , Vol. 24 ,pp. 105706, (2013).
54. X. Zhang, G. Guo, C. Ji, K. Huang, C. Zha, Y. Wang, L. Shen, A. Gupta, and N. Bao, Efficient Thermolysis Route to Monodisperse  $\text{Cu}_2\text{ZnSnS}_4$  Nanocrystals with Controlled Shape and Structure. *Scientific Reports*, Vol. 4 ,pp. 5086, (2014).
55. S. M. Camara, L. Wang, and X. Zhang, Easy Hydrothermal Preparation of  $\text{Cu}_2\text{ZnSnS}_4$  (CZTS) Nanoparticles for Solar Cell Application. *Nanotechnology*, Vol. 24, pp. 495401, (2013).
56. C. Rincon, and R. Marquez, Defect Physics of the  $\text{CuInSe}_2$  Chalcopyrite Semiconductor. *Journal of Physics and Chemistry of Solids*, Vol. 60, pp. 1865-1873, (1999).
57. S. H. Wei, and S. B. Zhang, Defect Properties of  $\text{CuInSe}_2$  and  $\text{CuGaSe}_2$ . *Journal of Physics and Chemistry of solids* ,Vol. 66 ,pp. 1994-1999, (2005).
58. S. H. Wei, S. B. Zhang, and A. Zunger, Effects of Ga Addition to  $\text{CuInSe}_2$  on its Electronic, Structural, and Defect Properties. *Applied physics letters*, Vol. 72, pp. 3199-3201, (1998).



59. S. Chen, A. Walsh, X. G. Gong and S. H. Wei, Classification of Lattice Defects in the Kesterite  $\text{Cu}_2\text{ZnSnS}_4$  and  $\text{Cu}_2\text{ZnSnSe}_4$  Earth-Abundant Solar Cell Absorbers. *Advanced materials*, 25, pp. 1522-1539, (2013).
60. S. Chen, A. Walsh, J. H. Yang, X. G. Gong, L. Sun, P. X. Yang, J. H. Chu, and S. H. Wei Compositional Dependence of Structural and Electronic Properties of  $\text{Cu}_2\text{ZnSn}(\text{S}, \text{Se})_4$  alloys for thin Film Solar Cells. *Physical Review B* ,Vol. 83, pp. 125201, (2011).
61. S. Chen, J. H. Yang, X. G. Gong, A. Walsh and S. H. Wei, Intrinsic Point D and Complexes in the Quaternary Kesterite Semiconductor  $\text{Cu}_2\text{ZnSnS}_4$ . *Physical Review B* ,Vol. 81 ,pp. 245204, (2010).
62. R. A. Wibowo, W. S. Kim, E. S. Lee, B. Munir and K. H. Kim, Single Step Preparation of Quaternary  $\text{Cu}_2\text{ZnSnSe}_4$  thin Films by RF Magnetron Sputtering from Binary Chalcogenide Targets. *Journal of Physics and Chemistry of Solids* ,Vol. 68 ,pp. 1908-1913, (2007).
63. M. Grossberg, J. Krustok, K. Timmo and M. Altsaar, Radiative Recombination in  $\text{Cu}_2\text{ZnSnSe}_4$  Monograins Studied by Photoluminescence Spectroscopy. *Thin Solid Films* ,Vol. 517, pp. 2489-2492, (2009).
64. T. Tanaka, T. Nagatom, D. Kawasaki, M. Nishio, Q. Guo, A. Wakahara, A. Yoshida, and H. Ogawa, Preparation of  $\text{Cu}_2\text{ZnSnS}_4$  thin Films by Hybrid Sputtering. *Journal of Physics and Chemistry of Solids* ,Vol. 66, pp. 1978-1981, (2005).
65. Y. Miyamoto, K. Tanaka, M. Oonuki, N. Moritake and H. Uchiki, Optical Properties of  $\text{Cu}_2\text{ZnSnS}_4$  thin Films Prepared by Sol–Gel and Sulfurization Method. *Japanese Journal of Applied Physics* ,Vol. 47S, pp. 596, (2008).
66. S. Chen, A. Walsh, Y. Luo, J. H. Yang, X. G. Gong and S. H. Wei, Wurtzite-Derived Polytypes of Kesterite and Stannite Quaternary Chalcogenide Semiconductors. *Physical Review B* ,Vol. 82, pp. 195203, (2010).
67. A. Nagoya, R. Asahi, R. Wahl and G. Kresse, Defect Formation and Phase Stability of  $\text{Cu}_2\text{ZnSnS}_4$  Photovoltaic Material. *Physical Review B* ,Vol. 81, pp. 113202, (2010).



68. S. Chen, L. W. Wang, A. Walsh, X. G. Gong, and S. H. Wei, Abundance of CuZn+SnZn and 2CuZn+SnZn Defect Clusters in Kesterite Solar Cells. *Applied Physics Letters*, Vol. 101, pp. 223901, (2012).
69. Y. Zhang, X. Sun, P. Zhang, X. Yuan, F. Huang and W. Zhang, Structural Properties and Quasiparticle Band Structures of Cu-based Quaternary Semiconductors for Photovoltaic Applications. *Journal of Applied Physics*, Vol. 111, pp. 063709, (2012).
70. J. Paier, R. Asahi, A. Nagoya, and G. Kresse, Cu<sub>2</sub>ZnSnS<sub>4</sub> as a potential photovoltaic material: A hybrid Hartree-Fock density functional theory study *Physical Review B*, vol. 79, pp. 115126, (2009).
71. E. A. Lund, H. Du, W. M. Hlaing, G. Teeter and M. A. Scarpulla, Investigation of Combinatorial Coevaporated thin Film Cu<sub>2</sub>ZnSnS<sub>4</sub> (II): Beneficial Cation Arrangement in Cu-rich growth. *Journal of Applied Physics*, Vol. 115, pp. 173503, (2014).
72. A. Shavel, M. Ibanez, Z. Luo, J. D. Roo, A. Carrete, M. Dimitrievska, A. Genc, M. Meyns, A. P. Rodriguez, M.V. Kovalenko, J. Arbiol and A. Cabot, Scalable Heating-up Synthesis of Monodisperse Cu<sub>2</sub>ZnSnS<sub>4</sub> Nanocrystals. *Chemistry of Materials*, Vol. 28, pp. 720-726, (2016).
73. P. Kush, S. K. Ujjain, N.C. Mehra, P. Jha, R. K. Sharma, S. Deka, Development and Properties of Surfactant-Free Water-Dispersible Cu<sub>2</sub>ZnSnS<sub>4</sub> Nanocrystals: a Material for low-Cost Photovoltaics. *ChemPhysChem*, Vol. 14, pp. 2793-2799, (2013).
74. A. Shavel, J. Arbiol, and A. Cabot, Synthesis of Quaternary Chalcogenide Nanocrystals: Stannite Cu<sub>2</sub>Zn<sub>x</sub>Sn<sub>y</sub>Se<sub>1+x+2y</sub>. *Journal of the American Chemical Society*, Vol. 132, pp. 4514-4515, (2010).
75. X. Song, X. Ji, M. Li, W. Lin, X. Luo and H. Zhang, A Review on Development Prospect of CZTS Based thin Film Solar Cells. *International Journal of Photoenergy*, Vol. 2014, (2014).
76. J. Y. Park, J. H. Noh, T. N. Mandal, S. H. Im, Y. Jun and S. Seok, Quaternary Semiconductor Cu<sub>2</sub>FeSnS<sub>4</sub> Nanoparticles as an Alternative to Pt Catalysts. *RSC Advances*, Vol. 3, pp. 24918-24921, (2013).



- 77.** Y. Cui, R. Deng, G. Wang and D. Pan, A General Strategy for Synthesis of Quaternary Semiconductor  $\text{Cu}_2\text{MSnS}_4$  ( $\text{M} = \text{Co}^{2+}, \text{Fe}^{2+}, \text{Ni}^{2+}, \text{Mn}^{2+}$ ) Nanocrystals. *Journal of Materials Chemistry*, Vol. 22, pp. 23136-23140, (2012).
- 78.** F. Lopez-Vergara, A. Galdamez, V. Manriquez, P. Barahona, O. Pena,  $\text{Cu}_2\text{Mn}_{1-x}\text{Co}_x\text{SnS}_4$ : Novel kesterite type solid solutions. *Journal of Solid State Chemistry*, Vol. 198, pp. 386-391, (2013).
- 79.** Y. Qi, Q. Tian, Y. Meng, D. Kou, Z. Zhou, W. Zhou, and S. Wu, Elemental Precursor Solution Processed  $(\text{Cu}_{1-x}\text{Ag}_x)_2\text{ZnSn}(\text{S},\text{Se})_4$  Photovoltaic Devices with over 10% Efficiency. *ACS applied materials & interfaces*, Vol. 9, pp.21243-21250, (2017).
- 80.** B. Murali, and S. B. Krupanidhi, Facile synthesis of  $\text{Cu}_2\text{CoSnS}_4$  nanoparticles exhibiting red-edge-effect: Application in hybrid photonic devices. *Journal of Applied physics*, Vol. 114, pp. 144312, (2013).
- 81.** S. Rondiya, N. Wadnerkar, Y. Jadhav, S. Jadkar, S. Haram, and M. Kabir, Structural, electronic, and optical properties of  $\text{Cu}_2\text{NiSnS}_4$ : a combined experimental and theoretical study toward photovoltaic applications. *Chemistry of Materials*, Vol. 29, pp 3133-3142, (2017).
- 82.** R. Pandey, R. Kumar, S. N. Sahu, and Suresh Chandra, *Handbook of Semiconductor Electrodeposition*. CRC Press, (2017).
- 83.** D. Lincot, Electrodeposition of semiconductors. *Thin Solid Films*, Vol. 487, pp. 40–48, (2005).
- 84.** D. Lincot, J. F. Guillemoles, S. Taunier, D. Guimard, J. Sicx-Kurdi, A. Chaumont, O. Roussel, O. Ramdani, C. Hubert, J. P. Fauvarque, N. Bodereau, L. Parissi, P. Panheleux, P. Fanouillere, N. Naghavi, P. P. Grand, M. Benfarah, P. Mogensen, and O. Kerrec Chalcopyrite thin film solar cells by electrodeposition. *Solar Energy*, Vol. 77, pp. 725–737, (2004).
- 85.** D. Cunningham, M. Rubcich, and D. Skinner, Cadmium telluride PV module manufacturing at BP solar. *Progress in Photovoltaics: Research and Applications*, Vol. 10, pp. 159–168, (2002).



86. B. E. McCandless, A. Mondal, and R. W. Birkmire, Galvanic deposition of cadmium sulfide thin films. *Solar Energy Materials and Solar Cells*, Vol. 36, pp. 369–379, (1995).
87. J. J. Scragg, P. J. Dale, and L. M. Peter, Towards sustainable materials for solar energy conversion: preparation and photoelectrochemical characterization of  $\text{Cu}_2\text{ZnSnS}_4$  *Electrochemistry Communications*, Vol. 10, pp. 639–642, (2008).
88. J. J. Scragg, P. J. Dale, L. M. Peter, G. Zoppi, and I. Forbes, New routes to sustainable photovoltaics: evaluation of  $\text{Cu}_2\text{ZnSnS}_4$  as an alternative absorber material. *Physica Status Solidi B*, Vol. 245, pp. 1772–1778, (2008).
89. J. J. Scragg, D. M. Berg, and P. J. Dale, A 3.2% efficient Kesterite device from electrodeposited stacked elemental layers. *Journal of Electroanalytical Chemistry*, Vol. 646, pp. 52–59, (2010).
90. H. Araki, Y. Kubo, A. Mikaduki, Preparation of  $\text{Cu}_2\text{ZnSnS}_4$  thin films by sulfurizing electroplated precursors. *Solar Energy Materials and Solar Cells*, Vol. 93, pp. 996–999, (2009).
91. H. Araki, Y. Kubo, K. Jimbo, Preparation of  $\text{Cu}_2\text{ZnSnS}_4$  thin films by sulfurization of co-electroplated Cu-Zn-Sn precursors. *Physica Status Solidi C*, Vol. 6, pp. 1266–1268, (2009).
92. R. Schurr, A. Hölzing, S. Jost, The crystallisation of  $\text{Cu}_2\text{ZnSnS}_4$  thin film solar cell absorbers from co-electroplated Cu-Zn-Sn precursors. *Thin Solid Films*, Vol. 517, pp. 2465–2468, (2009).
93. S. Ahmed, K. B. Reuter, O. Gunawan, L. Guo, L. T. Romankiw, and H. Deligianni, A high efficiency electrodeposited  $\text{Cu}_2\text{ZnSnS}_4$  solar cell. *Advanced Energy Materials*, Vol. 2, pp. 253–259, (2012).
94. N. M. Shinde, D. P. Dubal, D. S. Dhawale, C. D. Lokhande, J. H. Kim, and J. H. Moon, Room temperature novel chemical synthesis of  $\text{Cu}_2\text{ZnSnS}_4$  (CZTS) absorbing layer for photovoltaic application. *Materials Research Bulletin*, Vol. 47, pp. 302–307, (2012).
95. S. S. Mali, P. S. Shinde, C. A. Betty, P. N. Bhosale, Y. W. Oh, and P. S. Patil, Synthesis and characterization of  $\text{Cu}_2\text{ZnSnS}_4$  thin films by SILAR method. *Journal of Physics and Chemistry of Solids*, Vol. 73, pp. 735–740, (2012).



96. X. Miao, R. Chen, and W. Cheng, Synthesis and characterization of  $\text{Cu}_2\text{FeSnS}_4$  thin films prepared by electrochemical deposition. *Materials Letters*, Vol. 193, pp. 183-186, (2017).
97. H. Guan, H. Shen, B. Jiao, and X. Wang, Structural and optical properties of  $\text{Cu}_2\text{FeSnS}_4$  thin film synthesized via a simple chemical method. *Mater. Sci. Semicond. Process*, Vol. 25, pp. 159-162, (2014).
98. X. Meng, H. Deng, L. Sun, P. Yang, and J. Chu, Sulfurization temperature dependence of the structural transition in  $\text{Cu}_2\text{FeSnS}_4$ -based thin films. *Mater. Lett*, Vol. 161, pp. 427-430, (2015).
99. S. Zhang, CZTS thin film and its research progress of solar cell. *Engineering and Technology*, Vol. 8, pp. 67-69, (2010).
100. S. A. Vanalakar, G. L. Agwane, M. G. Gang, P. S. Patil, J. H. Kim, and J. Y. Kim, A mild hydrothermal route to synthesis of CZTS nanoparticle inks for solar cell applications. *Phys. Status Solidi C*, Vol. 12, pp. 500-503, (2015).
101. S. A. Vanalakar, V. L. Patil, P. S. Patil, and J. H. Kim, Controllable synthesis of stoichiometric  $\text{Cu}_2\text{ZnSnS}_4$  nanoparticles by solvothermal method and its properties. *AIP Conf. Proc*, Vol. 1665, pp. 050061, (2015).
102. C. An, K. Tang, G. Shen, C. Wang, L. Huang, and Y. Qian, The synthesis and characterization of nanocrystalline Cu- and Ag-based multinary sulfide semiconductors. *Mater. Res. Bull*, Vol. 38, pp. 823-830, (2003).
103. N. Muhunthan, O. Singh, S. Singh, and V. N. Singh, Growth of CZTS thin films by cosputtering of metal targets and sulfurization in  $\text{H}_2\text{S}$ . *International Journal of Photoenergy*, Vol. 2013, (2013).
104. K. Tanaka, Y. Fukui, N. Moritake, and H. Uchiki, Chemical Composition Dependence of Morphological and Optical Properties of  $\text{Cu}_2\text{ZnSnS}_4$  thin Films Deposited by Sol-Gel Sulfurization and  $\text{Cu}_2\text{ZnSnS}_4$  thin Film Solar Cell Efficiency. *Solar Energy Materials and Solar Cells*, Vol. 95, pp. 838-842, (2011).



- 105.** A. Ziti, B. Hartiti, S. Smariri, H. Labrim, Y. Nouri, A. Belafhaili, H. J. T. Nkuissi, S. Fadili, M. Tahri and P. Thevenin, Advancement of Stannite  $\text{Cu}_2\text{CoSnS}_4$  thin Films Deposited by Sol Gel Dip-Coating Route. *Physica Scripta*, Vol. 97, pp. 065815, (2022).
- 106.** Y. Zhao, W. Tao, X. Chen, J. Liu and A. Wei Synthesis and Characterization of  $\text{Cu}_2\text{ZnSnS}_4$  Nanocrystals Prepared by Microwave Irradiation Method *J. Mater. Sci.: Mater. Electron*, Vol. 26, pp. 5645–5651, (2015).
- 107.** H. Guan, Y. Shi, H. Hou, X. Wang and F. Yu, Quaternary  $\text{Cu}_2\text{CdSnS}_4$  Nanoparticles Synthesised by Microwave Irradiation Method. *Micro & Nano Letters*, Vol. 9, pp. 251-252, (2014).
- 108.** C. H. Lai, M. Yen Lu and L. J. Chen, Metal Sulfide Nanostructures: Synthesis, Properties and Applications in Energy Conversion and Storage. *Journal of Materials Chemistry*, Vol. 22, pp.19-30, (2012).
- 109.** M. G. Panthani, V. Akhavan, B. Goodfellow, J. P. Schmidtke, L. Dunn, A. Dodabalapur, P. F. Barbara and B. A. Korgel, Synthesis of  $\text{CuInS}_2$ ,  $\text{CuInSe}_2$ , and  $\text{Cu}(\text{In}_x\text{Ga}_{1-x})\text{Se}_2$  (CIGS) Nanocrystal inks for Printable Photovoltaics. *Journal of the American Chemical Society*, Vol. 130, pp. 16770-16777, (2008).
- 110.** P. Reiss, M. Protiere, and Liang Li. Core/shell Semiconductor Nanocrystals. *Small*, Vol. 5, pp.154-168, (2009).
- 111.** M. Konagai, M. Sugimoto, and K. Takahashi, High Efficiency GaAs thin Film Solar Cells by Peeled Film Technology. *Journal of crystal growth*, Vol. 45, pp. 277-280, (1978).
- 112.** J. J. Choi, Y. F. Lim, M. B. Santiago-Berrios, M. Oh, B. Hyun, L. Sun, A. C. Bartnik, A. Goedhart, G. G. Malliaras, H. D. Abruna, F. W. Wise and T. Hanrath, PbSe Nanocrystal Excitonic Solar Cells. *Nano letters*, Vol. 9, pp. 3749-3755, (2009).
- 113.** Y. Wu, C. Wadia, W. Ma, B. Sadtler and A. P. Alivisatos, Synthesis and Photovoltaic Application of Copper (I) Sulfide Nanocrystals. *Nano letters* ,Vol. 8 ,pp. 2551-2555, (2008).



- 114.** P. Kumar and K. Singh, Element Directed Aqueous Solution Synthesis of Copper Telluride Nanoparticles, Characterization, and Optical Properties. *Crystal Growth and Design*, Vol. 9, pp. 3089-3094, (2009).
- 115.** D. V. Talapin, A. L. Rogach, A. Kornowski, M. Haase, and H. Weller, Highly luminescent Monodisperse CdSe and CdSe/ZnS Nanocrystals Synthesized in a Hexadecylamine– Trioctylphosphine oxide– Trioctylphosphine Mixture. *Nano letters* , Vol. 1, pp. 207-211, (2001).
- 116.** R. Zeng, T. Zhang, J. Liu, S. Hu, Q. Wan, X. Liu, Z. Peng, and B. Zou, Aqueous Synthesis of Type-II CdTe/CdSe Core–Shell Quantum Dots for Fluorescent Probe labeling Tumor Cells. *Nanotechnology* ,Vol. 20 ,pp. 095102, (2009).
- 117.** S. Deka, A. Genovese, Y. Zhang, K. Miszta, G. Bertoni, R. Krahne, C. Giannini and L. Manna, Phosphine-Free synthesis of P-Type Copper (I) Selenide Nanocrystals in Hot Coordinating Solvents. *Journal of the American Chemical Society* ,Vol.132 ,pp. 8912-8914, (2010).
- 118.** L. Li, N. Coates, and D. Moses, Solution-Processed Inorganic Solar Cell Based on in Situ Synthesis and Film Deposition of CuInS<sub>2</sub> Nanocrystals, *Journal of the American Chemical Society* ,Vol. 132, pp. 22-23 ,(2010).
- 119.** G. J. Bauhuis, P. Mulder, E. J. Haverkamp, J. C. C. M. Huijben, J. J. Schermer, 26.1% thin-film GaAs solar cell using epitaxial lift-off. *Solar Energy Materials and Solar Cells*, Vol. 93, pp.1488-1491, (2009).
- 120.** S. Tamaki, W. T. Frankenberger Jr, Environmental biochemistry of arsenic. *Reviews of Environmental Contamination and Toxicology*, Vol. 124, pp. 79-110, (1992).
- 121.** M. Green, E. Dunlop, J. Hohl-Ebinger, M. Yoshita, N. Kopidakis and X.Hao, Solar Cell Efficiency Tables (version 57). *Progress in photovoltaics: research and applications*, Vol. 29, pp. 3-15, (2021).
- 122.** M. A. Green, K. Emery, Y. Hishikawa, W. Warta, E. D. Dunlop, D. H. Levi, and A. Ho-Baillie, Solar cell efficiency tables (version 49). *Progress in Photovoltaics: Research and Applications* Vol. 25, pp. 3-13, (2016).



- 123.** M. A. Green, K. Emery, Y. Hishikawa, W. Warta, and E. D. Dunlop, Solar cell efficiency tables (version 46). *Prog. Photovoltaics Res. Appl.* vol. 23, pp. 805–812, (2015).
- 124.** M. A. Green, K. Emery, Y. Hishikawa, W. Warta, and E. D. Dunlop, Solar cell efficiency tables (version 48). *Progress in Photovoltaics: Research and Applications*, vol. 24, pp. 905-913, (2016).
- 125.** [M. A. Green](#), [K. Emery](#), [D. L. King](#), S. Igari, and [Wilhelm Warta](#), Solar cell efficiency tables (version 26)., Vol. 13, pp. 387-392, (2005).
- 126.** M. A. Green, Y. Hishikawa, E. D. Dunlop, D. H. Levi, J. Hohl-Ebinger, and A. Ho-Baillie, Solar cell efficiency tables (version 52). *Progress in Photovoltaics: Research and Applications*, Vol. 26, pp. 427-436, (2018).
- 127.** S. K. Wallace, D. B. Mitzi, and A. Walsh, The Steady Rise of Kesterite Solar Cells. *ACS Energy Letters*, vol. 2, pp. 776–779, (2017).
- 128.** F. Zhang, and S. S. Wong, Controlled synthesis of semiconducting metal sulfide nanowires. *Chemistry of materials*, Vol. 21, pp. 4541-4554, (2009).
- 129.** Y. K. Albert Lau, D. J. Chernak, M. J. Bierman and S. Jin, Epitaxial growth of hierarchical PbS nanowires. *Journal of Materials Chemistry* ,Vol. 19, pp. 934-940, (2009).
- 130.** A. Singh, S. Singh, S. Levchenko, T. Unold, F. Laffir, and K. M. Ryan, Compositionally Tunable Photoluminescence Emission in  $\text{Cu}_2\text{ZnSn}(\text{S}_{1-x}\text{Se}_x)_4$  Nanocrystals. *Angewandte Chemie International Edition* ,Vol. 52, pp. 9120-9124, (2013) .
- 131.** Y. Yang, X. Kang, L. Huang and D. Pan, Tuning the band gap of  $\text{Cu}_2\text{ZnSn}(\text{S}, \text{Se})_4$  thin films via lithium alloying. *ACS Applied Materials & Interfaces* ,Vol. 8, pp. 5308-5313, (2016).
- 132.** D. B. Khadka and J. Kim, Structural transition and band gap tuning of  $\text{Cu}_2(\text{Zn}, \text{Fe})\text{SnS}_4$  chalcogenide for photovoltaic application. *The Journal of Physical Chemistry*, Vol. 118, pp. 14227-14237, (2014).



- 133.** S.C. Riha, B. A. Parkinson and Amy L. Prieto, Compositionally Tunable Cu<sub>2</sub>ZnSn (S<sub>1-x</sub>Sex)<sub>4</sub> Nanocrystals: Probing the Effect of Se-Inclusion in Mixed Chalcogenide Thin Films. *Journal of the American Chemical Society* ,Vol. 133, pp. 15272-15275 .(2011).
- 134.** F. Fan, L. Wu, M. Gong, G. Liu, Y. Wang, S. Yu, S. Chen, L. Wang and X. Gong, Composition-and Band-Gap-Tunable Synthesis of Wurtzite-Derived Cu<sub>2</sub>ZnSn (S<sub>1-x</sub>Sex)<sub>4</sub> Nanocrystals: Theoretical and Experimental Insights. *ACS nano* ,Vol. 7, pp. 1454-1463, (2013).
- 135.** K Yang, D. Son, S. Sung, J. Sim, Y. Kim, S. Park, D. Jeon, J. Kim, D. Hwang, C. Jeon, D. Nam, H. Cheong, J. Kang, and D. Kim, A band-gap-graded CZTSSe solar cell with 12.3% efficiency. *Journal of Materials Chemistry A*, Vol. 4, pp. 10151-10158, (2016).
- 136.** H. Zhou, W. Hsu, H. Duan, B. Bob, W. Yang, T. Song, C. Hsu and Y. Yang, CZTS nanocrystals: a promising approach for next generation thin film photovoltaics. *Energy & Environmental Science* ,Vol. 6, pp. 2822-2838, (2013).
- 137.** A. A. Rockett. Current status and opportunities in chalcopyrite solar cells. *Current Opinion in Solid State and Materials Science* ,Vol. 14, pp. 143-148 ,(2010).
- 138.** K. Sardashti, R. Haight, T. Gokmen, W. Wang, L. Chang, D. B. Mitzi, A. C. Kummel, Impact of nanoscale elemental distribution in high-performance kesterite solar cells. *Advanced Energy Materials* ,Vol. 5 ,pp. 1402180, (2015).
- 139.** W. Shockley, and H. J. Queisser, Detailed balance limit of efficiency of p-n junction solar cells. *Journal of applied physics* ,Vol. 32, pp. 510-519, (1961).
- 140.** W. Ki, and Hugh W. Hillhouse, Earth-abundant element photovoltaics directly from soluble precursors with high yield using a non-toxic solvent. *Advanced Energy Materials* ,Vol. 1 ,pp. 732-735, (2011).
- 141.** P. S. Maldar, M. A. Gaikwad, A. A. Mane, S. S. Nikam, S. P. Desai, S. D. Giri, A. Sarkar, A. V. Moholkar, Fabrication of Cu<sub>2</sub>CoSnS<sub>4</sub> thin films by a facile spray pyrolysis for photovoltaic application. *Solar Energy* ,Vol. 158, pp. 89-99, (2017).
- 142.** A. Sharma, and R. Thangavel, Cost-effective fabrication of Cu<sub>2</sub>CoSnS<sub>4</sub> thin films for photovoltaic applications. 2018 3rd International Conference on Microwave and Photonics (ICMAP). IEEE, (2018).



- 143.** A. Ziti, B. Hartiti, S. Smairi, H. Labrim, Y. Nouri, A. Belafhaili, H. T. Nkuissi, S. Fadili, M. Tahri and P. Thevenin, Advancement of stannite  $\text{Cu}_2\text{CoSnS}_4$  thin films deposited by sol gel dip-coating route. *Physica Scripta*, Vol. 97, pp. 065815, (2022).
- 144.** H. Hammami, M. Marzougui, H. Oueslati, M. BenRabeh, and M. Kanzari, Synthesis, growth and characterization of  $\text{Cu}_2\text{CoSnS}_4$  thin films via thermal evaporation method. *Optik*, Vol. 227, pp. 166054, (2021).
- 145.** P. S. Maldar, A. A. Mane, S. S. Nikam, S. D. Dhas, and A. V. Moholkar, Spray deposited  $\text{Cu}_2\text{CoSnS}_4$  thin films for photovoltaic application: effect of film thickness. *Thin Solid Films*, Vol. 709, pp. 138236, (2020).
- 146.** M. Beraich, M. Taibi, A. Guenbour, A. Zarrouk, M. Boudalia, A. Bellaouchou, M. Tabyaoui, S. Mansouri, Z. Sekkat, and M. Fahoume, Preparation and characterization of  $\text{Cu}_2\text{CoSnS}_4$  thin films for solar cells via co-electrodeposition technique: Effect of electrodeposition time. *Optik*, Vol. 193, pp. 162996, (2019).
- 147.** M. Rouchdi, E. Salmani, N. Hassanain and A. Mzerd, Effect of deposition time on structural and physical properties of  $\text{Cu}_2\text{CdSnS}_4$  thin films prepared by spray pyrolysis technique: experimental and ab initio study. *Optical and Quantum Electronics*, Vol. 49, pp. 1-12, (2017).
- 148.** A. Tombak, T. Kilicoglu, and Y. S. Ocak, Solar cells fabricated by spray pyrolysis deposited  $\text{Cu}_2\text{CdSnS}_4$  thin films. *Renewable Energy*, Vol. 146, pp. 1465-1470, (2020).
- 149.** Q. Xu, Z. Wang, H. Yang, Y. Xiang, G. Nie, and W. Yue, Synthesis of hierarchical  $\text{Cu}_2\text{CdSnS}_4$  by microwave-assisted transformation from precursor for photodegradation to malachite green. *Journal of Alloys and Compounds*, Vol. 904, pp. 163966, (2022).
- 150.** J. Zhou, S. Yu, X. Guo, L. Wu, and H. Li, Preparation and characterization of  $\text{Cu}_2\text{FeSnS}_4$  thin films for solar cells via a co-electrodeposition method. *Current Applied Physics*, Vol. 19, pp. 67-71, (2019).
- 151.** I. M. El Radaf, H. Y. S. Al-Zahrani, S. S. Fouad, and M. S. El-Bana, Profound optical analysis for novel amorphous  $\text{Cu}_2\text{FeSnS}_4$  thin films as an absorber layer for thin film solar cells. *Ceramics International*, Vol. 46, pp. 18778-18784, (2020).



- 152.** C. Nefzi, M. Souli, Y. Cuminal, and N. Kamoun-Turki, Effect of substrate temperature on physical properties of Cu<sub>2</sub>FeSnS<sub>4</sub> thin films for photocatalysis applications. *Materials Science and Engineering: B*, Vol. 254, pp. 114509, (2020).
- 153.** M. A. Abed, N. A. Bakr, and S. B. Mohammed, Synthesis and Characterization of Chemically Sprayed Cu<sub>2</sub>FeSnS<sub>4</sub> (CFTS) Thin Films: The Effect of Substrate Temperature. *Materials Science Forum*. Vol. 1039. Trans Tech Publications Ltd, (2021).
- 154.** M. Zaki, F. Sava, A. Buruiana, I. Simandan, N. Becherescu, A. Galca, C. Mihai, and A. Velea Synthesis and characterization of Cu<sub>2</sub>ZnSnS<sub>4</sub> thin films obtained by combined magnetron sputtering and pulsed laser deposition. *Nanomaterials*, vol. 11, pp. 2403, (2021).
- 155.** Y. Jayasree, Y.B. KishoreKumar, G. SureshBabu, P. UdayBhaskar, Growth of Cu<sub>2</sub>ZnSnS<sub>4</sub> thin films by hybrid chemical approach. *Physica B: Condensed Matter*, Vol. 618, pp. 413199, (2021).
- 156.** A. Murugan, V. Siva, A. Shameem, and S. AsathBahadur, Optimization of adsorption and reaction time of SILAR deposited Cu<sub>2</sub>ZnSnS<sub>4</sub> thin films: Structural, optical and electrochemical performance. *Journal of Alloys and Compounds*, Vol. 856, pp. 158055, (2021).
- 157.** A. A. Ahmad, A. B. Migdadi, A. M. Alsaad, I. A. Qattan, Qais M. Al-Bataineh, AhmadTelfah. Computational and experimental characterizations of annealed Cu<sub>2</sub>ZnSnS<sub>4</sub> thin films. *Heliyon*, Vol. 8, pp. e08683, (2022).
- 158.** M. A. Abed, N. A. Bakr, and J. Al-Zanganawee, Structural, Optical And Electrical Properties Of Cu<sub>2</sub>NiSnS<sub>4</sub> Thin Films Deposited By Chemical Spray Pyrolysis Method. *Chalcogenide Letters*, Vol. 17, pp. 179-186, (2020).
- 159.** A. Ziti, B. Hartiti, A. Belafhaili, H. Labrim, S. Fadili, A. Ridah, M. Tahri and P. Thevenin, Effect of dip-coating cycle on some physical properties of Cu<sub>2</sub>NiSnS<sub>4</sub> thin films for photovoltaic applications. *Journal of Materials Science: Materials in Electronics*, Vol. 32, pp. 16726-16737, (2021).



- 160.** H.Hussein, and A.Yazdani, Spin-coated Cu<sub>2</sub>CrSnS<sub>4</sub> thin film: A potential candidate for thin film solar cells. *Materials Science in Semiconductor Processing*, Vol. 91, pp. 58-65, (2019).
- 161.** S. M. Abdullah, N. A. Bakr, S. A. Salman, Structural, Optical, and Electrical, Properties of Ag<sub>2</sub>ZnSnS<sub>4</sub> Sprayed Thin Films by Chemical Pyrolysis Method. *Chalcogenide Letters*, Vol. 18, pp. 65-73, (2021).
- 162.** W. Wang, M. T. Winkler, O. Gunawan, T. Gokmen, T. K. Todorov, Y. Zhu, and D. Mitzi, Device characteristics of CZTSSe thin film solar cells with 12.6% efficiency, *Adv. Energy Mater*, Vol. 4, pp. 201301465, (2014).
- 163.** K. Sun, C. Yan, F. Liu, J. Huang, F. Zhou, J. A. Stride, M. Green, and X. Hao, Over 9% efficient kesterite Cu<sub>2</sub>ZnSnS<sub>4</sub> solar cell fabricated by using Zn<sub>1-x</sub>CdxS buffer layer. *Advanced Energy Materials*, Vol. 6, pp. 1600046, (2016).